Magnetic Resonance Imaging of Bone Marrow: A Review – Part I

David T. Wang, D.O.

Division of Musculoskeletal Imaging, Wilford Hall Ambulatory Surgical Center, San Antonio, TX

Bone marrow is a complex organ containing undifferentiated cells from which the various constituents of blood originate. Under the control of hormones, cytokines and growth factors, normal marrow is susceptible to proliferation or suppression secondary to multiple influences, to include infection, medications, radiation, toxins, neoplasms, and nutritional deficiencies, among others. While histopathologic examination is the primary means for evaluating bone marrow, detection of marrow abnormality often occurs during medical imaging.

In part I of our review, the normal MRI appearance of bone marrow and its pattern of maturation from birth to adulthood will be discussed. We will then discuss disease processes characterized by marrow depletion, followed by a discussion of treatment-related marrow changes and marrow conditions which are not otherwise easily categorized. In part II of our review, bone marrow edema, myeloproliferative disease, marrow infiltration and replacement, and marrow ischemia will be covered in detail.

Normal Marrow

Normal bone marrow is composed of variable proportions of hematopoietic cells and fat. The proportion of each fluctuates over time depending on age and homeostatic requirements. These cells are set upon a framework of trabecular bone, perfused by a rich sinusoidal network of capillaries, and innervated by a neuroreticular complex of myelinated and unmyelinated neural fibers. The complex and dynamic process of bone remodeling is the result of a delicate balance of osteoblast and osteoclast activity. These processes are further supported by a cadre of reticuloendothelial cells, stromal cells, macrophages, lymphocytes, and plasma cells.^{2,3}

The natural progression from birth to adulthood is a gradual shift from predominantly cellular or

"red marrow," to a mixture of predominantly fatty or "yellow marrow," a process termed "marrow conversion." With aging, there is a concomitant decline in the number of trabeculae. The shift toward predominantly fatty marrow follows a predictable pattern, occurring first in the appendicular skeleton followed by the axial skeleton. The process is usually completed by 25 years of age.

MRI evaluation of bone marrow exploits compositional differences between red and yellow Hematopoietically active red marrow marrow. contains 40% water, 40% fat, and 20% protein, while yellow marrow contains 15% water, 80% fat, and 5% protein.² Because of the greater fat content, yellow marrow has hyperintense signal intensity on T1 and fast spin-echo T2-weighted sequences, intermediate signal on spin-echo T2 sequences, and signal drop out on fat suppressed sequences.4 While red marrow contains some fat, its higher cellular content results in relative hypointense signal compared to yellow marrow on T1 weighted images (but higher signal intensity than muscle), and intermediate to slightly hyperintense signal relative to yellow marrow on fluid sensitive MR sequences.⁴ Because MRI has such exquisite sensitivity in discerning the differences in marrow composition, the fatty component of marrow is often detected earlier in younger patients than would be expected by macroscopic histologic inspection.^{5,6}

Marrow Conversion in the Appendicular Skeleton

The conversion of red to yellow marrow is a dynamic phenomenon that occurs in a predictable, orderly, symmetrical and centripetal pattern. All Marrow conversion begins in the distal aspect of the extremities (hands and feet) and extends proximally to involve the long bones of the extremities. Within individual long bones, marrow

conversion follows a centrifugal pattern with replacement of red marrow by fatty marrow beginning in the shafts of long bones before progressing to the ends of bone. Marrow conversion in the long bones of the forearm and lower leg can lag slightly behind the femora and humeri. Many authors characterize the progression of marrow conversion into four distinct stages: infantile, childhood, adolescent, and adult patterns; A,8-11 however, variation has been observed with marrow conversion in the femur occurring earlier than expected in some subjects. 12

Infantile marrow (newborn up to one year):

Normal marrow in late fetal and early infant life is characterized by a high concentration of red marrow throughout the axial and appendicular skeleton. Thus, the diaphyses and metaphyses of long bones on MRI have low T1 signal, while unossified epiphyses and apophyses composed predominantly of cartilage exhibit intermediate signal on T1 weighted images (figs. 1 and 2).^{5,13} Later, when epiphyses and apophyses ossify, yellow marrow becomes evident within the ossification centers as areas of hyperintense T1 signal.

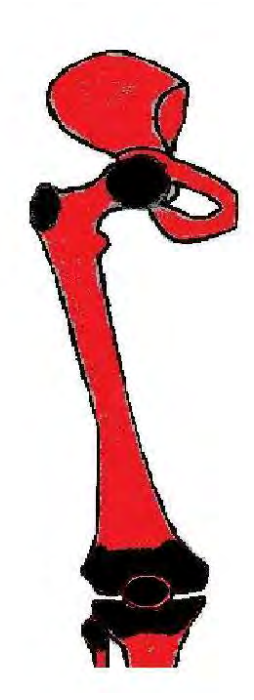


Figure 1. Schematic diagram of the infantile marrow (just after birth) showing global distribution of red marrow . (Red areas represent red marrow and black areas represent cartilage).



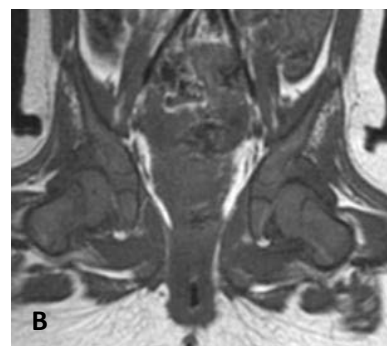


Figure 2. Sagittal T1 weighted image of the knee in a 18 day old male (A) shows hypointense red marrow in the proximal tibial (and distal femoral) metadiaphyses (white arrow) and intermediate signal (isointense to muscle) in the cartilaginous epiphyses (black arrow). Coronal T1 weighted image of the pelvis in an 8 month old male (B) shows hypointense red marrow throughout the proximal femurs and pelvis.

Childhood marrow (one year to 10 years):

Near the end of the first year of life, marrow conversion begins in the phalanges of the hands and feet and is complete by 1 year of age. Additionally, marrow conversion in the femoral diaphyses commences by 12 months of age, sometimes seen as early as 3 months of age. ¹⁰ After the first year of life, yellow marrow replaces red marrow in the diaphyses, while red marrow remains within the metaphyses. This results in relatively hyperintense signal in the diaphyses and low to intermediate signal intensity in the metaphyses on T1 weighted sequences (figs. 3 and 4).²



Figure 3. Schematic diagram of childhood marrow (1-10 years) showing yellow marrow distributed in apophyses, epiphyses, and the diaphysis and red marrow situated in the proximal and distal metaphyses. (Red areas denote red marrow, yellow areas denote yellow marrow, and black areas denote cartilage).



Figure 4. Coronal T1 weighted image of the pelvis in a 20 month old male. Note hyperintense yellow marrow within the ossification centers of the femoral and tibial epiphyses (white arrows), intermediate to hypointense signal of the unossified cartilaginous epiphyses (black arrow), and the intermediate to low marrow signal of red marrow in the metaphyses (red arrow).

Adolescent marrow (10 years to 25 years):

In the second decade of life, continued conversion of predominantly red marrow to predominantly yellow marrow in the diaphyses of long bones is accompanied by recession of red marrow from the distal metaphyses. Thus, there is a slightly greater proportion of yellow marrow in the distal metaphyses, resulting in progressively increasing hyperintense signal on T1 weighted images (figs. 5 and 6).



Figure 5. Schematic diagram of adolescent marrow (10-20 years) showing recession of red marrow from the distal metaphysis and replacement of yellow marrow in the diaphysis and distal metaphysis. (Red areas denote regions of red marrow and yellow areas denote regions of yellow marrow).

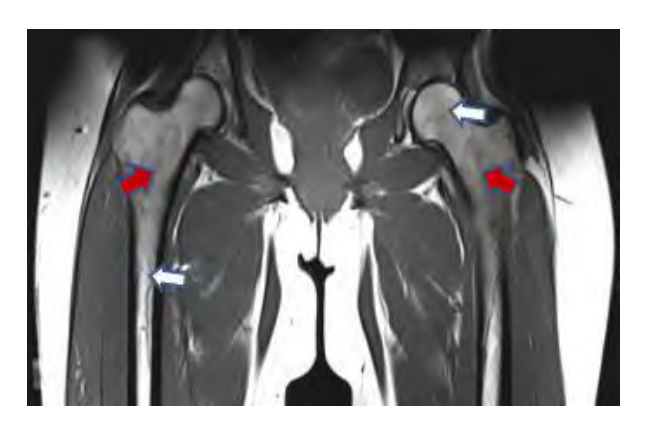


Figure 6. Coronal T1 weighted image of the pelvis in an 18-year-old female. Note hyperintense yellow marrow within the femoral epiphyses and diaphyses (white arrows) and intermediate to low marrow signal of red marrow in the proximal femoral metaphysis.

Adult marrow (over 25 years):

By the middle of the third decade, the mature or adult pattern of marrow is achieved with yellow predominating throughout marrow appendicular skeleton, except for the proximal metaphyses of the femora and humeri (figs. 7 and 8). In the proximal femur, marrow conversion has been further characterized by Ricci's group who reported 4 distinct patterns with progressive loss of red marrow from the medial femoral neck, a phenomenon they proposed was related to mechanical stress.8 Eventually, complete recession of red marrow from the proximal femoral metaphyses develops later in life, occurring as early as 35 years of age in men and 55 years of age in women.4 This results in a near homogeneous hyperintense signal on T1 weighted images (fig. 8).



Figure 7. Schematic diagram of adult distribution of marrow (over 25 years) showing yellow marrow throughout the femur except for the proximal metaphysis. (Red areas denote red marrow and yellow areas denote yellow marrow)

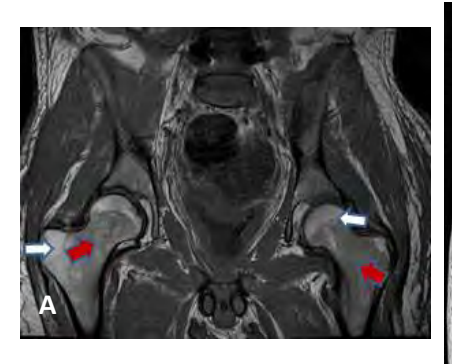




Figure 8. Coronal T1 image in a 28-year-old male (A) shows areas of red marrow in the proximal femoral metaphyses (red arrows) and pelvis and fatty marrow in the epiphyses and trochanters (white arrows). Coronal T1 image in a 91-year-old male (B) shows diffuse yellow marrow.

Marrow Conversion in the Axial Skeleton

The axial skeleton includes the spine, ribs, sternum, skull, and pelvis. It serves as a repository of red marrow throughout life, with marrow conversion occurring much slower and to a lesser extent than in the appendicular skeleton.

In the spine, the pattern of marrow conversion often is less predictable. Ricci's group described 4 patterns of marrow in the spine among varying age groups. In their study, the majority of subjects in the youngest group (ages less than 20) demonstrated a pattern of diffuse homogenously hypointense T1 signal within the vertebral bodies with linear hyperintense signal along the upper and lower margins of the basivertebral veins. Therefore, early in life, widespread red marrow results in lower signal intensity than adjacent intervertebral discs on T1 weighted images (Fig. 9).

In older groups of patients, Ricci noted variable distribution of the other 3 marrow patterns: (a) peripheral band-like and triangular areas of hyperintense signal adjacent to endplates and involving the anterior and posterior vertebral body corners; (b) punctate and/or patchy heterogeneous hyperintense signal; or (c) a combination of these two. These patterns varied from one region of the spine to another. Nevertheless, the expected pattern of marrow conversion in adulthood is from predominantly red marrow to a greater proportion of yellow marrow, resulting in hyperintense T1 marrow signal relative to adjacent intervertebral discs (Fig. 10).⁸



Figure 9. Sagittal T1 weighted image of the thoracic spine in an 8-day-old male. Note the relative hypointensity of the vertebral bodies (red arrow) compared to the slightly hyperintense intervertebral discs (white arrow).



Figure 10. Sagittal T1 weighted image of the lumbar spine in a 76-year-old male shows near homogeneous hyperintense marrow signal compatible with fatty marrow.

Like the spine, the pattern of marrow conversion in the pelvis is less drastic than in the appendicular skeleton. Through the second decade of life, the pelvis is largely filled with red marrow, homogeneous until the age of 1. Over time, islands of yellow marrow arise in the acetabulum and anterior ilium. A Ricci's group reported 2 marrow patterns in the pelvis, both of which were marked by a predominant pattern of red marrow. One

pattern is seen in younger patients with small areas of yellow marrow in the acetabulum superior and medial to the hip joint; the second pattern is seen in older patients with additional areas of yellow marrow in the ilium and adjacent to the sacroiliac joints. While the majority of the literature on marrow conversion focuses on age related differences, the sacrum is one area where gender related differences were identified. Duda's group found higher fat content in the sacral lateral masses in male subjects compared to females in a group of subjects 17-42 years old. 15

Marrow Reconversion

When the supply of blood cells is insufficient to maintain homeostasis, the body is able to upregulate blood cell production through marrow reconversion. Reconversion refers to red marrow proliferation or hyperplasia in areas where yellow marrow had become the dominant component. This pattern follows the reverse order as the observed in marrow pattern conversion. Specifically, resurgence of red marrow occurs in an overall centripetal manner, from the axial to the appendicular skeleton. The appearance of red marrow in individual long bones begins in the proximal metaphyses, followed by the distal metaphyses, and finally the diaphyses. The bones of the hands and feet are last to undergo marrow reconversion. Epiphyses may also be recruited for hematopoiesis, though usually only when the demand for blood cells is extreme. 16,17

Increased demand for blood cell production can result in hyperplasia as a physiologic response in patients with severe chronic anemia (sickle cell, thalassemia, hereditary spherocytosis), patients treated with granulocyte colony stimulating factor during chemotherapy, overweight female smokers, people living at high altitudes, and marathon runners (Figs 11, 12, 13).^{2,7,18-20} Unfortunately, marrow hyperplasia can also be seen in patients with underlying marrow replacement disease, such as lymphoma, leukemia, and metastases, which can confound the evaluation. Because of this, the MR characteristics of hyperplasic marrow can be difficult to differentiate from pathologic infiltration and vice versa.²¹

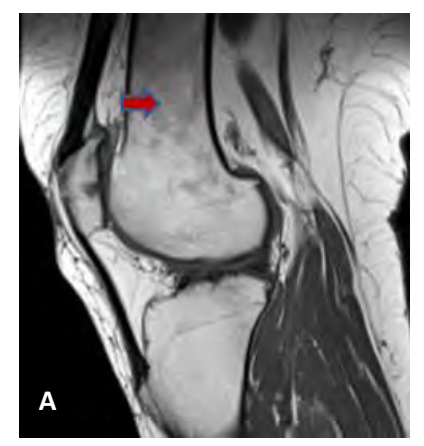
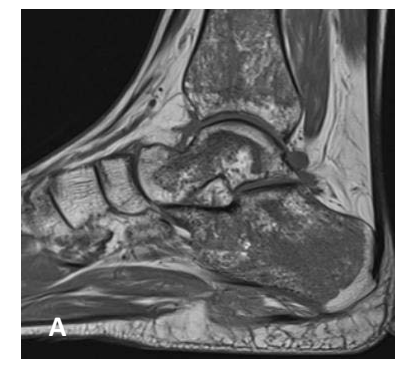




Figure 11. Sagittal T1 (A) and fat suppressed T2 (B) images show areas of red marrow in the distal femur in a 62 year old obese female nonsmoker (red arrows). Note the signal intensity of marrow is slightly hyperintense on T1 and T2 images compared to adjacent muscle.



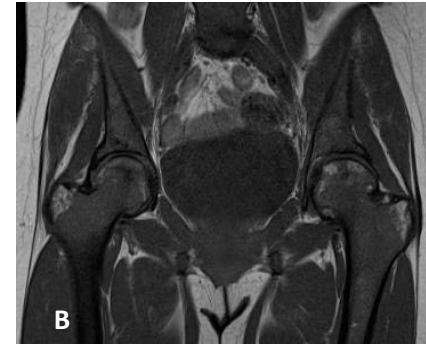


Figure 12. Sagittal T1 image of the foot/ankle (A) shows patchy areas of hypointense marrow reconversion in a 22-year-old female with sickle cell anemia. Coronal T1 image of the pelvis (B) in the same patient reveals diffuse red marrow with the exception of fatty marrow within the epiphyses and trochanters. Crescentic regions of hypointense signal in the femoral heads is consistent with avascular necrosis.



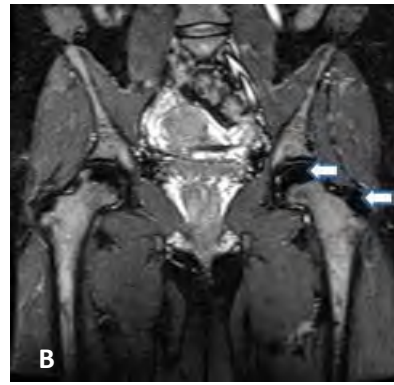


Figure 13. Coronal T1 (A) and T2 weighted with fat suppression (B) images of the pelvis show diffuse hypointense T1 and hyperintense T2 marrow reconversion in a 37-year-old female treated with chemotherapy for breast cancer. Fatty marrow remains within the epiphyses and trochanters (white arrows).

A few useful discriminators favoring benign marrow hyperplasia include symmetric involvement, signal intensity of red marrow equal to that of normal muscle on STIR and fat suppressed T2 weighted images, and lack of aggressive features such as cortical destruction. Reconverted marrow will show intermediate signal on T1, T2, and STIR sequences in a nonconfluent patchy pattern. 7,22

In contrast, pathologic marrow infiltration tends to have hypointense T1 and hyperintense T2 signal relative to muscle. Therefore, T1 signal intensity less than or equal to that of muscle or intervertebral discs should prompt the radiologist to consider causes of abnormal marrow signal other than hematopoietic marrow. Because nonneoplastic hyperplastic marrow does not replace normal marrow elements (namely fat) as is expected with most neoplastic processes, opposed-phase imaging may have some utility in discriminating benign from pathologic marrow. Lastly, in those that are equivocal, short interval follow up with MRI or bone marrow biopsy are reasonable approaches.

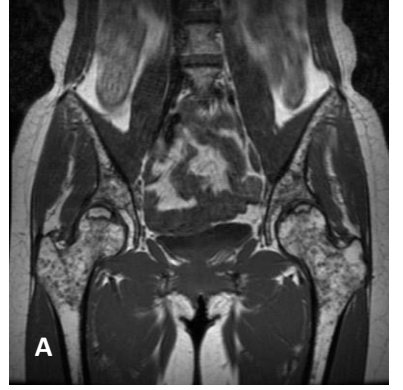
Marrow Depletion

When the body fails to upregulate hematopoiesis to maintain homeostasis and the overall amount of red marrow elements becomes depressed, this is termed marrow depletion. Histologic evaluation of marrow depletion reveals hypocellular or acellular marrow on a background of diffuse fatty replacement, or predominantly yellow marrow. This pattern of abnormal marrow can be seen following treatment with chemotherapy or radiation, as well as with aplastic anemia of any cause. While diagnosis of marrow depletion is usually made with serological evaluation, medical imaging is useful for evaluation of recurrent disease or to evaluate response to therapy in the case of aplastic anemia.

Aplastic Anemia:

The earliest description of aplastic anemia was by Erlich in 1888 who published a case of a young pregnant woman who presented with bleeding, fever, and severe anemia. She was found to have marrow largely devoid of blood-forming elements at autopsy.²⁵ Aplastic anemia is a relatively rare condition characterized bγ anemia pancytopenia on peripheral smear (decreased circulating blood elements) and hypocellularity of the bone marrow (decreased progenitor cells). Aplastic anemia can be inherited (Fanconi anemia), acquired, or idiopathic. While the majority of cases are idiopathic, the list of acquired causes includes toxins (benzene), medications (Chloramphenicol, Carbamazepine, Phenytoin), infection (parvovirus and viral hepatitis), and radiation chemotherapy treatment. Aplastic anemia has also been associated with connective tissue disease (systemic lupus erythematosus) and pregnancy.

On MRI, aplastic marrow tends to have diffusely hyperintense T1 signal because of predominantly fatty marrow. This is most conspicuous in areas typically dominated by red marrow, such as the spine and pelvis (Fig. 14). Occasionally, aplastic marrow can appear heterogeneous on T1 weighted sequences with areas of patchy low signal corresponding to foci of fibrosis. During treatment, myeloid elements may begin to return and T1 weighted images will show scattered small islands of hypointense signal corresponding to foci of resurgent red marrow.²⁶ This appearance can be confused with areas of fibrosis, neoplasm, or myelodysplastic disease.



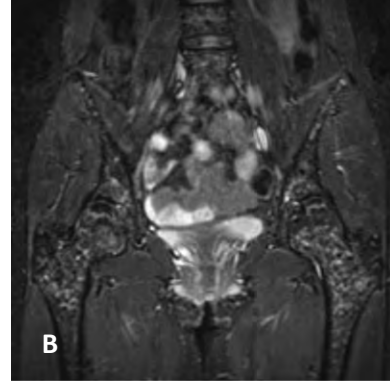


Figure 14. Coronal T1 and STIR images in a 39-year-old female with aplastic anemia show diffuse fatty infiltration of the marrow with patchy areas of low T1 signal. Note the crescentic areas of low signal in the femoral epiphyses consistent with avascular necrosis.

Radiation:

The medical uses of ionizing radiation include the treatment of various cancers, such as multiple

myeloma and metastatic disease. An anticipated side effect of radiation therapy is marrow suppression. Myeloid elements, being the more sensitive component of marrow, are damaged and destroyed before fatty or yellow marrow. degree of red marrow injury and its ability to replenish damaged cells is dependent upon radiation treatment dose, volume of marrow treatment frequency.²⁷ treated, and irradiation with doses in the range of 3-45 Gy result in rapid bone marrow alteration which may persist up to 2 years.²⁸ Regeneration of bone marrow is expected with local radiation doses below 30 Gy, while doses above 50 Gy will result in marrow ablation.²⁹

Following radiation, the earliest changes detected by MRI have been observed within 3 weeks, and as early as eight days. 30,31 MRI demonstrates hyperintense signal on STIR images, which is thought to reflect bone marrow edema, hemorrhage, and possibly an influx of unirradiated cells. 11 weighted images in the first few days appear normal. The pattern of increased signal on STIR images decreases over time between the third and sixth week after treatment. At this point marrow signal on T1 weighted images increases, corresponding to predominantly fatty marrow. After the sixth week, the majority of affected patients will have hyperintense T1 signal (fatty marrow) that can last up to 2 years (Fig. 15). 28,32

In the spine, two "late" patterns of marrow depletion following radiation have been described on T1 sequences: (a) homogeneous pattern of diffusely increased signal, and (b) "band" pattern with a peripheral region of intermediate signal intensity bordering a central zone of hyperintense signal. Irradiated marrow typically has a conspicuous appearance on T1 weighted images with hyperintense fatty marrow confined to the expected area of a radiation portal demarcated by a sharp line. Marrow changes outside the radiation portal have also been reported. 31,33,34

Chemotherapy:

Similar to radiation, the goal of chemotherapy in the treatment of marrow disease is marrow ablation. Early after chemotherapy, marrow appears hypointense on T1 weighted images and hyperintense on fat-suppressed T2 and STIR images owing to marrow congestion. Over time, with destruction of the myeloid elements and increasing fatty deposition, the marrow will show hyperintense T1 signal. Failure to observe this pattern can provide a clue to the radiologist that there is treatment failure or disease relapse. If the chemotherapy regimen includes granulocyte-colony stimulating factor (G-CSF), fatty transformation can be delayed or reflect a pattern of marrow reconversion which can confound evaluation for disease relapse or treatment efficacy. ³⁵

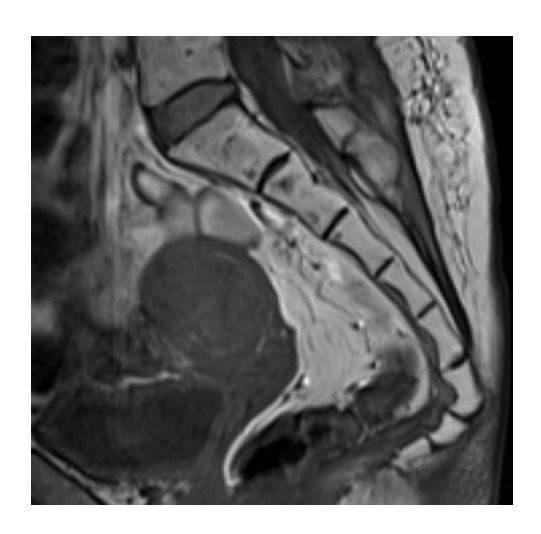


Figure 15. Sagittal T1 image of the sacrum in a 45-year-old female post radiation and chemotherapy for rectal carcinoma shows diffuse fatty marrow signal 8 months after radiation therapy.

Other Marrow Diseases

While the majority of marrow conditions fall within larger categories (marrow depletion, proliferation, replacement, infiltration, edema and ischemia), there are some conditions which are difficult to categorize but deserve mention among miscellaneous conditions.

Osteopetrosis:

Osteopetrosis is a hereditary skeletal dysplasia characterized by abnormal osteoclastic activity, resulting in a generalized pattern of diffusely increased bone density. Four distinct subtypes have been described: precocious or "infantile" (autosomal recessive and lethal), delayed (autosomal dominant and mild), intermediate (autosomal recessive), and tubular acidosis type

calcifications).36 cerebral (with characteristic osteoclastic activity affects remodeling such that there is poor cortical and medullary differentiation, leading undertubularization, metaphyseal widening, and dense metaphyseal bands. Despite the increase in density, bones are structurally weak and prone to fracture. Classically, there is a "bone within a bone" appearance, which in the spine has been described as the "sandwich" vertebra sign. Abnormal remodeling of cranial nerve foramina can result in deafness and blindness.

On MRI, the typical appearance of osteopetrosis is that of diffuse sclerotic bone with diffusely hypointense signal on T1 and T2 weighted images (Fig. 16). This appearance is nonspecific and can be seen with hemosiderosis, diffuse blastic metastases, or fibrosis.³⁷

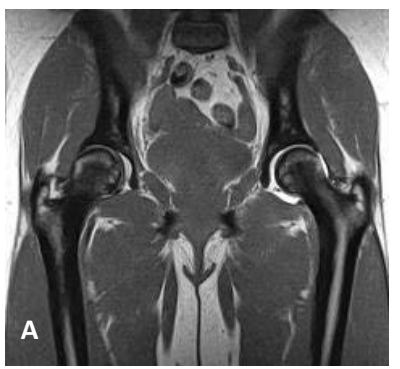




Figure 16. Coronal T1 (A) and STIR (B) MR images through the pelvis show marked cortical thickening with diffusely low signal on the T1 weighted image and narrowing of the marrow space, which contains relatively hyperintense red marrow on STIR (red arrow).

Paget Disease:

Paget disease is commonly seen in men over 40 years of age and of European descent. Hallmark radiographic features include bony expansion with trabecular and cortical thickening. While its cause is poorly understood, the disease is thought to be related to an imbalance of osteoclastic and osteoblastic activity. It is characterized by three phases of the disease: (a) purely lytic, (b) mixed lytic and blastic, and (c) purely blastic. While the diagnosis of Paget disease is typically made on the basis of the radiographic appearance, MRI can be useful in the evaluation for complications of Paget

disease, to include osteomyelitis, sarcomatous degeneration, giant cell tumor formation (skull), and metastases to hypervascular Pagetic bone.

The MRI appearance is variable but thought to reflect the state of the marrow as it is influenced by the various phases of disease, which can occur simultaneously. Early disease without significant marrow disturbance will appear normal with the exception of decreased size of the marrow space due to cortical thickening. Between the lytic and mixed phases (which are considered the more active phases), the marrow space appears heterogeneous on T1 and T2 weighted images (Fig. 17). This is likely related to deposition of fibrovascular tissue, which appears hypointense on T1 but hyperintense on T2 weighted images because of granulation tissue and slow blood flow through vascular channels.³⁸ Other foci of hyperintense signal on T1 are possibly related to areas of fatty filled marrow spaces. 38 Unfortunately, the MRI appearance can be nonspecific and resemble that of infection or neoplasm.





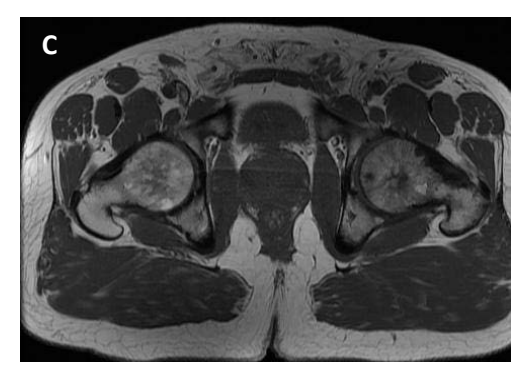
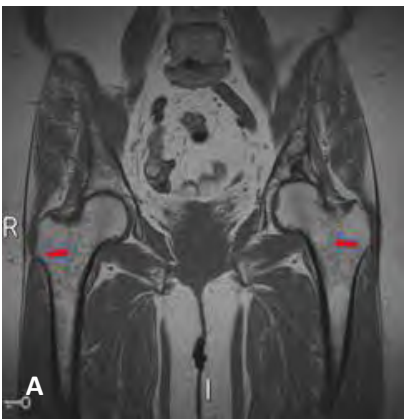


Figure 17. Coronal T1 (A), coronal fat suppressed T2 (B), and axial proton density (C) weighted images of the pelvis in a 49-year-old man with Paget disease. Note the bony expansion and coarsened trabecular thickening of the left femur.

Gaucher Disease:

The most common of the lysosomal storage diseases, Gaucher disease is characterized by a deficiency of glucocerebrosidase, which results in abnormally high levels of glucocerebroside that is taken up by histiocytes (termed Gaucher cells).³⁹ Proliferation of Gaucher cells ensues with accumulation of glycolipids throughout the reticuloendothelial system. Within the marrow, this ultimately leads to cellular necrosis, fibrous proliferation, and loss of spongy trabeculae.³⁶ Expansion of the marrow space by lipid-laden Gaucher cells results in the Erlenmeyer flask deformity of the femora. Additionally, there is generalized osteoporosis with progressive weakening of subchondral bone, predisposing affected patients to fracture. Vertebral fractures may manifest as vertebra plana or an H-shaped vertebra, similar to that seen in sickle cell disease.^{36,40} Elsewhere, weakening of the bone and osteonecrosis can be a nonspecific finding indistinguishable from other causes of avascular necrosis.

On MRI, Gaucher disease is nonspecific with patchy heterogeneous hypointense signal on T1 and T2 weighted images, similar to that seen in marrow infiltrative disease. With osteonecrosis, there may be areas of hyperintense T2 signal acutely which later become hypointense when necrosis is chronic (Fig. 18).



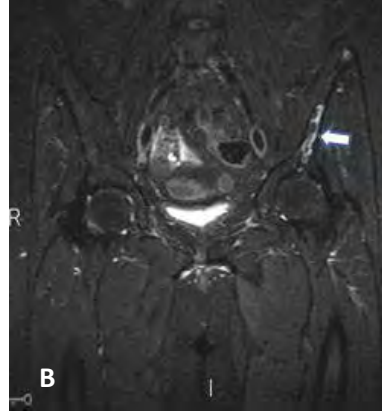
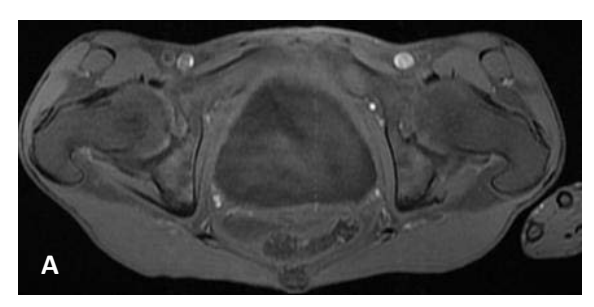


Figure 18. Coronal T1 (A) and STIR (B) images of the pelvis in a middle-aged female with Gaucher disease. Note the heterogeneous marrow pattern with areas of low signal in the proximal femora on the T1 weighted image (red arrows - A) and the areas of bone marrow infarction in the left ilium on the fat suppressed T2 weighted image (white arrow - B).

Iron Storage Disease:

Deposition of iron in marrow occurs in conditions where there is increased breakdown of erythrocytes (such as sickle cell anemia or thallassemia), iron overload (as in those who are on chronic blood transfusion therapy), or when there is overall abnormal absorption (such as in primary hemochromatosis). Common to all is a diffuse pattern of marked hypointense marrow signal on both T1 and T2 weighted images with blooming artifact on T2 gradient echo imaging.



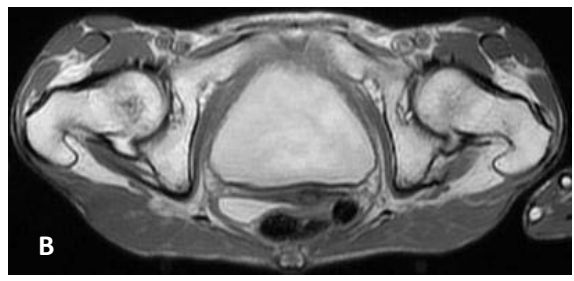


Figure 19. Axial T1 (A) and fat suppressed T2 (B) images of the pelvis in a young adult female with anorexia nervosa show diffusely hypointense T1 and hyperintense T2 marrow signal intensity, consistent with serous atrophy of bone marrow. Note how marrow signal follows the signal intensity of urine. Images courtesy of Ryan Fajardo, MD.

Serous Atrophy or Gelatinous Transformation:

In patients with profound loss of body fat stores, as in patients who have severe cachexia, anorexia nervosa, or acquired immunodeficiency syndrome, a phenomenon known as serous atrophy or gelatinous transformation of the bone marrow can occur. Histologic descriptions of the marrow in these patients show a gray-pink gelatinous or serous marrow that contains atrophied fat and hematopoietic cells set on a matrix rich in hyaluronic acid. This watery matrix results in marked hyperintense signal intensity on T2 weighted images with hypointense signal on T1 weighted images (Fig. 19). The process may be

focal or diffuse.⁴² Furthermore, the progression of disease mimics the pattern observed with normal marrow conversion, namely transformation begins in the hands and feet, followed by the long bones of the distal arms and legs, before finally affecting the spine and pelvis.

Summary

In conclusion, interpretation of marrow on MRI requires an understanding of the normal pattern of marrow maturation or conversion, as well as an understanding of how the hematopoietic and fatty constituents of marrow contribute to the normal MRI appearance. Knowledge of the normal appearance of marrow allows for recognition of pathologic marrow processes. In part I of this review, we discussed marrow conversion and reconversion, as well as disorders of marrow depletion and important but miscellaneous processes which are otherwise difficult to categorize. In part II of our review, additional marrow conditions such as bone marrow edema, infiltration, and replacement; myeloproliferative disease; and marrow ischemia will be discussed.

The views expressed in this material are those of the author, and do not reflect the official policy or position of the U.S. Government, the Department of Defense, or the Department of the Air Force.

References

- 1. Travlos GS. Normal Structure, Function, and Histology of the Bone Marrow. Toxicologic Pathology 2006; 34:548-565.
- 2. Vogler JB, Murphy WA. Bone Marrow Imaging. Radiology 1988; 168:679-693.
- 3. Abboud CN, Lichtman MA. Structure of the marrow and the hematopoietic microenvironment. In: Williams Hematology, Eighth Edition (K Kaushansky, MA Lichtman, E Beutler, TJ Kipps, U Seligsohn, JT Prchal, eds) McGraw-Hill, New York, 2010.
- 4. Vande berg BC, Malghem J, Lecouvet FE, Maldague B. Magnetic resonance imaging of the normal bone marrow. Skeletal Radiology 1998; 27:471-483.
- 5. Moore SG, Dawson KL. Red and yellow marrow in the femur: age-related changes in appearance at MR imaging. Radiology 1990; 175:219-223.
- 6. Moore SG, Bisset GS, Siegel MJ, Donaldson JS. Pediatric Musculoskeletal MR Imaging. Radiology 1991; 179:345-360.
- 7. Andrews CL. Evaluation of the Marrow Space in the Adult Hip. Radiology 2000; 20:S27-S42.
- 8. Ricci C, Cova M, Kang YS, Yang A, Rahmouni A. Scott MW. Zerhouni EA. Normal Age-Related Patterns of Cellular and Fatty Bone Marrow Distribution in the Axial Skeleton: MR Imaging Study. Radiology 1990; 177:83-88.

- 9. Vande berg BC, Malghem J, Lecouvet FE, Maldague B. Magnetic Resonance imaging of normal bone marrow. European Radiology 1998;8:1327-1334.
- 10. Guillerman RP. Chapter 177 Imaging of Normal and Abnormal Bone Marrow. Caffey's Pediatric Diagnostic Imaging, 11th edition. Thomas L. Slovis ed, 2008 Mosby Elsevier, Philadelphia
- 11. Hwang S, Panicek DM. Magnetic Resonance Imaging of Bone Marrow in Oncology, Part I. Skeletal Radiology 2007;36:913-920.
- 12. Waitches G, Zawin JK, Poznanski AK. Sequence and Rate of Bone Marrow Conversion in the Femora of Children as Seen on MR Imaging: Are Accepted Standards Accurate? Am J Roentgenol. 1994 Jun;162(6):1399-406.
- 13 .Foster K, Chapman S, Johnson K. MRI of the marrow in the paediatric skeleton. Clinical Radiology 2004; 58:651-673.
- 14. Siegel MJ, Luker GD. Bone marrow imaging in children. Magn Reson Imaging Clin N Am. 1996 Nov:4(4)771-96.
- 15. Duda SH. Laniando M, Schick F, Strayle M, Claussen CD. Normal Bone Marrow in the Sacrum of Young Adults: Difference Between the Sexes Seen on Chemical-Shift MR Imaging. AJR 1995; 164:935-940
- 16. Steiner RM, Mitchell DF, Rao VM, et al. Magnetic resonance imaging of bone marrow: diagnostic value in diffuse hematologic disorders. Magn Reson Q 1990;6:17-34.
- 17. Mirowitz SA, Hematopoietic bone marrow within the proximal humeral epiphysis in normal adults: investigation with MR imaging. Radiology. 1993 Sep;188(3):689-93.
- 18. Poulton TB, Murphy WD, Duerk JL, Chapek CC, Feiglin DH. Bone marrow reconversion in adults who are smokers: MR Imaging findings. Am J Roentgenol. 1993 Dec;161(6):1217-21.
- 19. Deutsch AL, Mink JH, Rosenfelt FP, Waxman AD. Incidental detection of hematopoietic hyperplasia on routine knee MR imaging. Am J Roentgenol. 1989 Feb;152(2):333-6.
- 20. Siegel MJ. "MRI of Bone Marrow." ARRS. Retrieved 11/21/2011;http://www.google.com/url?sa=t&rct=j&q=mri%20 of%20bone%20marrow%20siegel&source=web&cd=1&ved=0C CYQFjAA&url=http%3A%2F%2Fwww.arrs.org%2FshopARRS%2F products%2Fpdf.cfm%3FtheFile%3Ds06p_sample.pdf&ei=V-rJToaWJs-k2gWjvZXXDw&usg=AFQjCNG-
- Xr_uFnrXQ8DPiS3A9cnsHQHLgg.
- 21. Bordalo-Rodrigues M, Galant C, Lonneux M, Clause D, Vande Berg BC. Focal nodular hyperplasia of the hematopoietic marrow simulating vertebral metastasis on FDG positron emission tomography. AJR Am J Roentgenol. 2003 Mar;180(3):669-71.
- 22. Caldemeyer KS, Smith RR, Harris A, Williams T, Huang Y, Eckert GJ, Slemenda CW. Hematopoietic bone marrow hyperplasia: correlation of spinal MR findings, hematologic parameters, and bone mineral density in endurance athletes. Radiology. 1996 Feb;198(2):503-8.
- 23. Vande Berg BC, Lecouvet FE, Galant C, Maldague BE, Malghem J. Normal Variants and Frequent Marrow Alterations that Simulate Bone Marrow Lesions at MR Imaging. Radiol Clin N Am 2005; 43:761-770.
- 24. Carroll KW, Feller JF, Tirman PF. Useful internal standards for distinguishing infiltrative marrow pathology from hematopoietic marrow at MRI. J Magn Reson Imaging. 1997 Mar-Apr;7(2):394-8.

- 25. Ehrlich P. Uber einen Fall von Anamie mit Bemerkungen uber regenerative Veranderungen des Knochenmarks. Charite-Annalen 1888;13:300
- 26. Kaplan PA, Asleson RJ, Klassen LW, Duggan MJ.Bone marrow patterns in aplastic anemia: observations with 1.5-T MR imaging. Radiology. 1987 Aug;164(2):441-4.
- 27. Sacks EL, Goris ML, Glatstein E, Gilbert E, Kaplan HS. Bone marrow regeneration following large field radiation: influence of volume, age, dose, and time. Cancer. 1978 Sep;42(3):1057-65.
- 28. Ramsey RG, Zacharias CE.MR imaging of the spine after radiation therapy: easily recognizable effects.AJR Am J Roentgenol. 1985 Jun;144(6):1131-5.
- 29. Casamassima F, Ruggiero C, Caramella D, Tinacci E, Villari N, Ruggiero M.Hematopoietic bone marrow recovery after radiation therapy: MRI evaluation.Blood. 1989 May 1;73(6):1677-81.
- 30. Stevens SK, Moore SG, Kaplan ID. Early and late bone-marrow changes after irradiation: MR evaluation. AJR Am J Roentgenol. 1990 Apr;154(4):745-50.
- 31. Blomlie V, Rofstad EK, Skjønsberg A, Tverå K, Lien HH.Female pelvic bone marrow: serial MR imaging before, during, and after radiation therapy.Radiology. 1995 Feb;194(2):537-43.
- 32. Yankelevitz DF, Henschke CI, Knapp PH, Nisce L, Yi Y, Cahill P.Effect of radiation therapy on thoracic and lumbar bone marrow: evaluation with MR imaging. AJR Am J Roentgenol. 1991 Jul;157(1):87-92.
- 33. Otake S, Mayr NA, Ueda T, Magnotta VA, Yuh WT. Radiation-induced changes in MR signal intensity and contrast enhancement of lumbosacral vertebrae: do changes occur only inside the radiation therapy field? Radiology. 2002 Jan;222(1):179-83.

- 34. Kauczor HU, Dietl B, Brix G, Jarosch K, Knopp MV, van Kaick G. Fatty replacement of bone marrow after radiation therapy for Hodgkin disease: quantification with chemical shift imaging. J Magn Reson Imaging 1993; 3:575–580
- 35. Fletcher BD, Wall JE, Hanna SL. Effect of hematopoietic growth factors on MR images of bone marrow in children undergoing chemotherapy.Radiology. 1993 Dec;189(3):745-51.
- 36. McAlister WH, Herman TE. Osteochondrodysplasias, Dysostoses, Chromosomal Aberrations, Mucopolysaccharidoses, and Mucolipidoses. In: Bone and Joint Imaging, Third Edition (Resnick D, Kransdorf MJ, eds) Elsevier Saunders, Philadelphia, PA, 2005.
- 37. Rao VM, Dalinka MK, Mitchell DG, Spritzer CE, Kaplan F, August CS, Axel L, Kressel HY. Osteopetrosis: MR characteristics at 1.5 T. Radiology. 1986 Oct;161(1):217-20.
- 38. Roberts MC, Kressel HY, Fallon MD, Zlatkin MB, Dalinka MK. Paget disease: MR imaging findings. Radiology. 1989 Nov;173(2):341-5.
- 39. Cotran RS, Kumar V, Collins T. Robbins Pathologic Basis of Disease Sixth Edition. Saunders, Philadelphia, PA, 1999,
- 40. Manaster BJ, Disler DG, May DA. Musculoskeletal Imaging The Requisites, Second Edition. Mosby, Saint Louis, MO, 2002.
- 41. Vande Berg BC, Malghem J, Lecouvet FE, Lambert M, Maldague BE. Distribution of serouslike bone marrow changes in the lower limbs of patients with anorexia nervosa: predominant involvement of the distal extremities. AJR Am J Roentgenol. 1996 Mar;166(3):621-5.
- 42. Vande Berg BC, Malghem J, Devuyst O, Maldague BE, Lambert MJ. Anorexia nervosa: correlation between MR appearance of bone marrow and severity of disease. Radiology. 1994 Dec;193(3):859-64.